Heliyon 10 (2024) e31751

Contents lists available at ScienceDirect

Heliyon

journal homepage: www.cell.com/heliyon

Research article

# Association of clinical and imaging characteristics with pulmonary function testing in patients with Long-COVID

Lin-Mei Zhao [b,c], Andrew C. Lancaster [b,d], Ritesh Patel [b], Helen Zhang [f], Tim Q. Duong [e], Zhicheng Jiao [f], Cheng Ting Lin [b], Terrance Healey [f], Thaddeus Wright [f], Jing Wu [a,*], Harrison X. Bai [b]

[a] Department of Radiology, The Second Xiangya Hospital, Central South University, Changsha, Hunan, China
[b] Department of Radiology and Radiological Science, Johns Hopkins University School of Medicine, Baltimore, MD, USA
[c] Department of Radiology, Xiangya Hospital, Central South University, Changsha, Hunan, China
[d] Johns Hopkins University School of Medicine, Baltimore, MD, USA
[e] Department of Radiology, Albert Einstein College of Medicine and Montefiore Medical Center, Bronx, NY, USA
[f] Department of Diagnostic Imaging, Rhode Island Hospital, Providence, RI, USA

ARTICLE INFO

*Keywords:*
CT
COVID-19
Pulmonary function test

ABSTRACT

*Purpose:* The purpose of this study is to identify clinical and imaging characteristics associated with post-COVID pulmonary function decline.

*Methods:* This study included 22 patients recovering from COVID-19 who underwent serial spirometry pulmonary function testing (PFT) before and after diagnosis. Patients were divided into two cohorts by difference between baseline and post-COVID follow-up PFT: Decline group (>10 % decrease in FEV1), and Stable group (≤10 % decrease or improvement in FEV1). Demographic, clinical, and laboratory data were collected, as well as PFT and chest computed tomography (CT) at the time of COVID diagnosis and follow-up. CTs were semi-quantitatively scored on a five-point severity scale for disease extent in each lobe by two radiologists. Mann-Whitney U-tests, T-tests, and Chi-Squared tests were used for comparison. P-values <0.05 were considered statistically significant.

*Results:* The Decline group had a higher proportion of neutrophils (79.47 ± 4.83 % vs. 65.45 ± 10.22 %; p = 0.003), a higher absolute neutrophil count (5.73 ± 2.68 × $10^9$/L vs. 3.43 ± 1.74 × $10^9$/L; p = 0.031), and a lower proportion of lymphocytes (9.90 ± 4.20 % vs. 21.21 ± 10.97 %; p = 0.018) compared to the Stable group. The Decline group also had significantly higher involvement of ground-glass opacities (GGO) on follow-up chest CT [8.50 (4.50, 14.50) vs. 3.0 (1.50, 9.50); p = 0.032] and significantly higher extent of reticulations on chest CT at time of COVID diagnosis [6.50 (4.00, 9.00) vs. 2.00 (0.00, 6.00); p = 0.039] and follow-up [5.00 (3.00, 13.00) vs. 2.00 (0.00, 5.00); p = 0.041]. ICU admission was higher in the Decline group than in the Stable group (71.4 % vs. 13.3 %; p = 0.014).

*Conclusions:* This study provides novel insight into factors influencing post-COVID lung function, irrespective of pre-existing pulmonary conditions. Our findings underscore the significance of neutrophil counts, reduced lymphocyte counts, pulmonary reticulation on chest CT at diagnosis, and extent of GGOs on follow-up chest CT as potential indicators of decreased post-COVID lung function. This knowledge may guide prediction and further understanding of long-term sequelae of COVID-19 infection.

* Corresponding author. Department of Radiology The Second Xiangya Hospital of Central South University Changsha, China.
*E-mail address:* wujing622@csu.edu.cn (J. Wu).

https://doi.org/10.1016/j.heliyon.2024.e31751
Received 28 September 2023; Received in revised form 20 May 2024; Accepted 21 May 2024
Available online 22 May 2024
2405-8440/© 2024 Published by Elsevier Ltd. This is an open access article under the CC BY-NC-ND license (http://creativecommons.org/licenses/by-nc-nd/4.0/).

**Abbreviations**

| | |
|---|---|
| ANC | Absolute Neutrophil Count |
| BMI | Body Mass Index |
| CBC | Complete Blood Count |
| CT | Chest Computed Tomography |
| $FEF_{25-75}$ | Forced Expiratory Flow Between 25 % and 75 % |
| $FEV_1$ | Forced Expiratory Volume in 1 Second |
| FVC | Forced Vital Capacity |
| GGO | Ground-Glass Opacities |
| ICC | Interclass Correlation Coefficients |
| ILD | Interstitial Lung Disease |
| NE | Neutrophil Elastase |
| PACS | Picture Archiving and Communication System |
| PFT | Pulmonary Function Testing |
| RBC | Red Blood Cell |
| $SpO_2$ | Oxygen Saturation |
| TGF | Transforming Growth Factor |

## 1. Introduction

In the aftermath of the height of the COVID-19 pandemic, some individuals continue to grapple with lingering symptoms long after their initial recovery, a phenomenon termed long-COVID [1–5]. Pulmonary complications stand out prominently among the observed sequelae [6,7]. Notably, there is evidence that individuals with pre-existing pulmonary conditions appear to face an increased risk of exacerbation of their preexisting condition and clinical deterioration following COVID-19 infection [8–10]. Despite extensive research efforts carried out thus far to better characterize long-COVID through symptomatology [11,12], spirometry pulmonary function testing (PFT) [13,14], and chest computed tomography (CT) [14–19], a critical gap persists in understanding the longitudinal changes in lung function and their correlation with radiological findings post-COVID, since the availability of longitudinal data for lung function is limited.

Furthermore, follow-up studies focusing on longitudinal CT changes of long-COVID have reported the presence of fibrotic features in some cases [12,20], whereas others have not observed such findings [21]. Additionally, variability in ground-glass opacity (GGO) abnormalities across studies has been noted [22,23], suggesting a potential progression of underlying lung pathology previously undetected [24]. Therefore, there is an unresolved debate surrounding the origin of diminished pulmonary function following infection - whether it arises primarily from pre-existing conditions or as a direct consequence of COVID-19 infection. This uncertainty underscores the need for comprehensive investigation to elucidate the trajectory of lung function following COVID-19 and its relationship with pre-existing pulmonary health.

It's worth noting that in patients who undergo serial PFT evaluations for underlying stable disease, a comparison between worsening vs. stable PFT trajectories post-COVID may provide insight into characteristics associated with clinical worsening and help predict which individuals will experience pulmonary sequelae. Therefore, to reduce the potential confounding impact of pre-existing pulmonary conditions, we sought to study a unique cohort of individuals with COVID-19 in whom serial PFTs demonstrated clinical stability prior to the diagnosis of COVID-19. This study's primary aim is to identify demographic, laboratory, and imaging traits present at the time of COVID-19 diagnosis that are associated with the subsequent decline in pulmonary function post-COVID.

## 2. Materials and methods

This study received Institutional Review Board (IRB) approval with a waiver of informed consent from each study participant (IRB00329311).

### 2.1. Subjects, definitions/criteria

This study represents a single-center clinical case series. A retrospective electronic medical record review was performed for all patients seen at a Johns Hopkins hospital with suspected COVID-19 from 2020 to 2022. The inclusion criteria for participants were as follows: 1. COVID-19 diagnosis using microbiologically-detected SARS-CoV-2 RNA; 2. Baseline (time of COVID-19 diagnosis) and follow-up chest CT; 3. Pre-baseline, baseline, and follow-up spirometry PFT; 4. Stable pulmonary function (less than 10 % change in percent predicted forced expiratory volume in 1 s [$FEV_1$ (% predicted)]) between pre-baseline and baseline PFT, to decrease the likelihood of any decrease in pulmonary function on follow-up PFT unrelated to COVID-19. Patients who met the following exclusion criteria were excluded from the study: 1. Long interval (over 3.5 years) [25] between baseline PFT/chest CT and time of COVID-19 diagnosis; 2. Long interval (over 1 year) [26] between baseline/follow-up PFT and respective chest CT; 3. Short interval (less than 3 months) [27] between baseline PFT/CT and follow-up PFT/CT, respectively; 4. Unstable pulmonary function (over 10 % change in

$FEV_1$ [% predicted]) between pre-baseline and baseline PFT. Detailed information regarding inclusion and exclusion criteria is provided in Fig. 1. Subjects were then split into two cohorts: Decline group and Stable group. The Decline group was defined as subjects with a >10 % decrease in percent predicted $FEV_1$ on follow-up PFT compared to baseline PFT. Conversely, the Stable group was defined as subjects with a ≤10 % decrease or improvement in percent predicted $FEV_1$ between baseline and follow-up PFT. Time intervals between PFTs and COVID-19 diagnosis are provided in Supplementary Table 1. PFT results over time and PFT parameters of the two groups are provided in Fig. 2 and Supplementary Table 2.

### 2.2. Data collection

Demographic, PFT, CT, clinical, and laboratory data were collected for all participants. Data for subject age, gender, race, smoking status, alcohol use, body mass index (BMI), oxygen saturation ($SpO_2$%), ICU admission, ventilator use, and corticosteroid treatment at the time of diagnosis were collected (Table 1). In addition, presenting symptoms of COVID-19 disease (Table 2) and history of comorbidities at time of COVID-19 diagnosis (Supplementary Table 3) were collected. Clinical indication for pre-baseline PFT prior to COVID-19 diagnosis was also documented (Supplementary Table 4). Baseline and follow-up PFT parameters included forced vital capacity (FVC), percentage of predicted FVC [FVC (% predicted)], forced expiratory volume in 1 s ($FEV_1$), percentage of predicted $FEV_1$ [$FEV_1$ (% predicted)], $FEV_1$/FVC (%), percentage of predicted $FEV_1$/FVC [$FEV_1$/FVC (% predicted)], forced expiratory flow between 25 % and 75 % ($FEF_{25-75}$), percentage of predicted $FEF_{25-75}$ [$FEF_{25-75}$ (% predicted)] (Supplementary Table 2). Percent predicted $FEV_1$ was used for group assignment as described previously. Laboratory blood test results at the time of COVID-19 diagnosis are shown in Table 3.

Chest CT/CTA data were retrospectively pulled from the Picture Archiving and Communication System (PACS) and de-identified. Baseline and follow-up chest CTs were independently scored semi-quantitatively on a five-point severity scale for disease extent in each lobe (0 = 0 % lung involvement; 1 = <5 %; 2 = 5–25 %; 3 = 26–50 %; 4 = 51–75 %; 5 = >75 %) by two radiologists (LZ and RP), based on a system proposed by Francone et al. [28]. The averages of the readers' scores for each lobe were used in analysis, and the CT score was defined as the sum of the lobar scores (0–25). CTs were assessed for presence of ground-glass opacities, traction bronchiectasis, subpleural curvilinear opacities, reticulations, consolidations, and honeycombing (Table 4 and Table 5).

### 2.3. Statistical analysis

All statistical analyses were performed on IBM SPSS Statistics software (SPSS, 26.0.0.0). The Kolmogorov-Smirnov test was used to determine whether a continuous variable follows a Normal Distribution. For parameters with a p-value less than 0.05 from the test, further evaluation was conducted using a normal P–P plot and a histogram. Continuous variables that follow a normal distribution are denoted using Mean ± Standard Deviation (SD), while non-normally distributed continuous variables are represented using Median

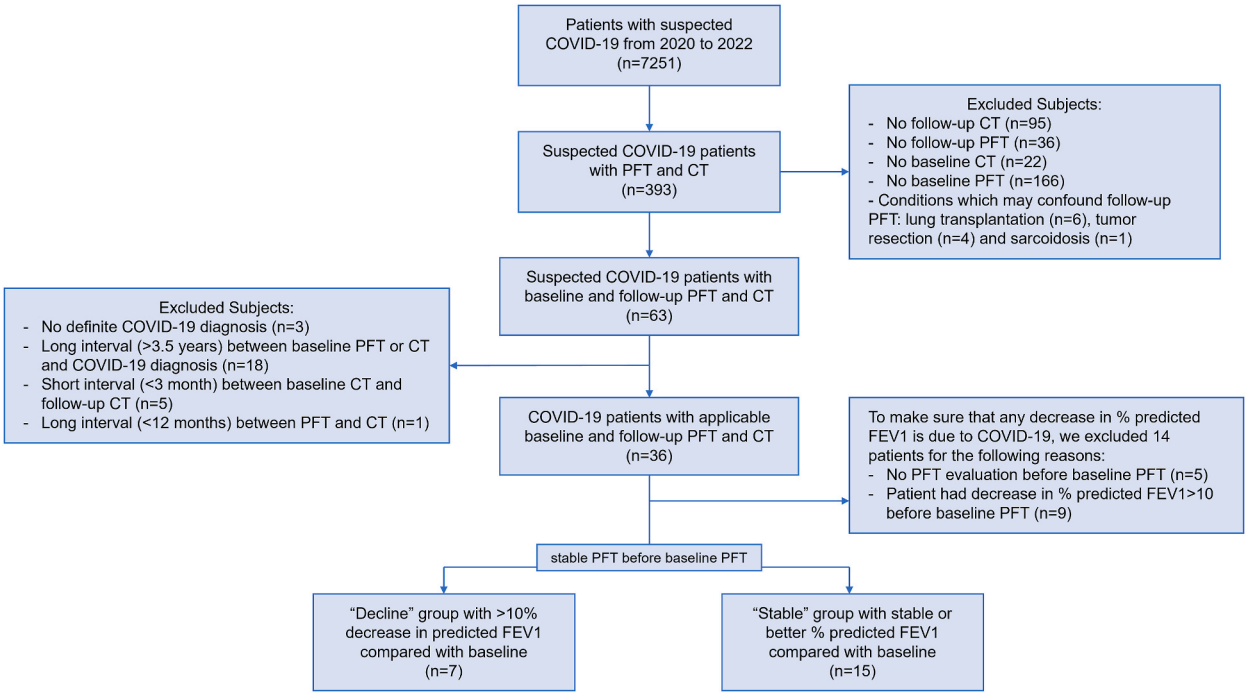


**Fig. 1.** Flowchart of participant enrollment.
PFT = Pulmonary Function Testing, CT = Computed Tomography.

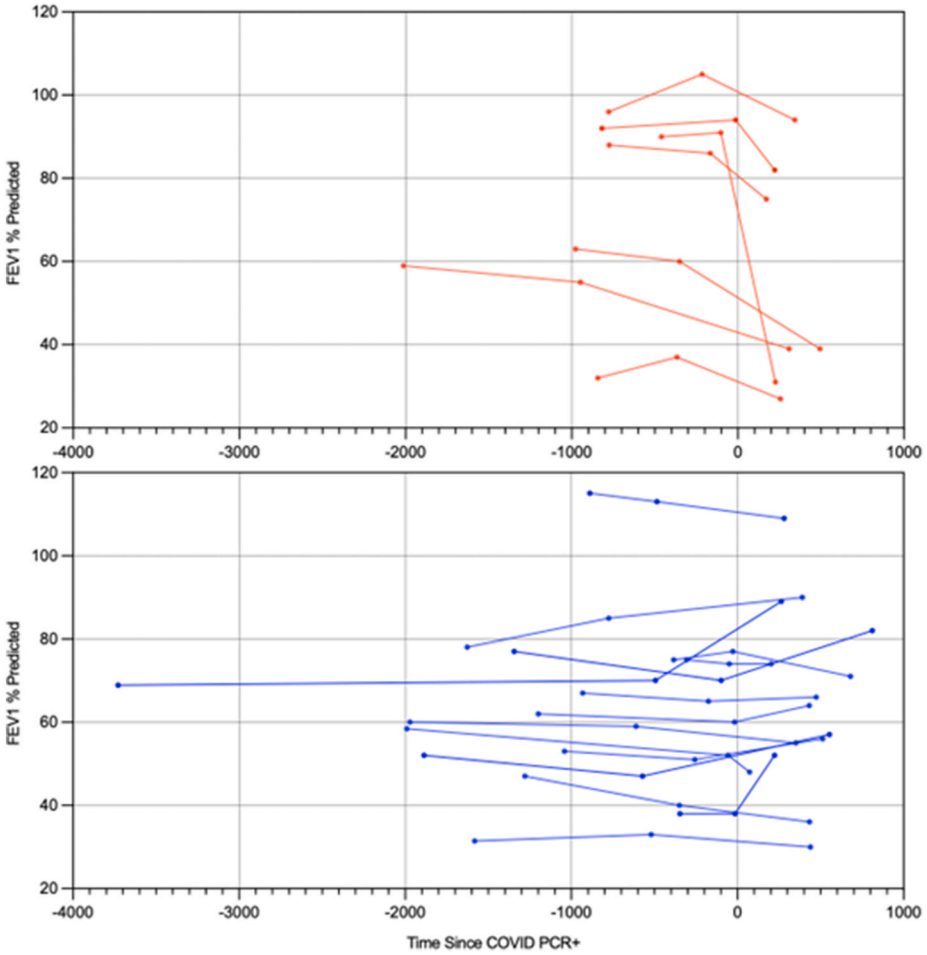


**Fig. 2.** $FEV_1$ % predicted at different time points in relation to COVID-19 diagnosis. The red denotes the Decline group with decreased $FEV_1$ % predicted, and the blue represents the Stable group with stable or increased $FEV_1$ % predicted.

and Interquartile Range (IQR). Discrete variables are represented using Count (Percentage [%]). Mann-Whitney U-tests, independent t-tests, and Chi-Squared tests were used to compare the Decline and Stable groups. Paired t-tests were used for comparison between baseline and follow-up CT evaluations. Interclass correlation coefficients (ICC) were used to evaluate consistency between the two radiologists. P-values less than 0.05 were considered statistically significant.

## 3. Results

### 3.1. Decline and Stable group demographics

Twenty-two subjects were included in this study, 7 in the Decline group and 15 in the Stable group. The cohorts did not differ significantly in age (years, Decline: 69.71 ± 9.73, Stable: 62.8 ± 15; $p = 0.281$), gender ($p = 1.000$), race ($p = 0.071$), smoking status ($p = 0.384$), alcohol use ($p = 0.267$), BMI ($p = 0.712$), $SpO_2$ at admission ($p = 0.581$), ventilator usage during hospitalization ($p = 0.361$), corticosteroid treatment ($p = 0.135$) (Table 1) or indications for PFTs prior to COVID-19 diagnosis (from $p = 0.274$ to $p = 1.000$, depending on indication). There were also no significant differences between the cohorts in symptoms (from $p = 0.101$ to $p = 1.000$) (Table 2) or comorbidities (from $p = 0.161$ to $p = 1.000$) present at admission (Supplementary Table 3). There was a significant difference observed in the percentage of subjects requiring a higher level of care during hospitalization, with 71.4 % (n = 5) of the Decline group and 13.3 % (n = 2) of the Stable group admitted to an ICU ($p = 0.014$) (Table 1). The indications for serial PFT tests are shown in Supplementary Table 4.

### 3.2. Laboratory testing

Laboratory testing revealed a significantly higher proportion of neutrophils (79.47 ± 4.83 % vs. 65.45 ± 10.22 %; $p = 0.003$),

**Table 1**
Demographic, ICU admission, and ventilator use data for Decline and Stable groups at time of COVID-19 diagnosis.

| Characteristics | Decline Group (n = 7) | Stable Group (n = 15) | p-value |
|---|---|---|---|
| Age (years) | 69.71 ± 9.73 | 62.80 ± 15.00 | 0.281 |
| Gender | | | 1.000 |
| Male (n, %) | 3 (42.9) | 6 (40.0) | |
| Female (n, %) | 4 (57.1) | 9 (60.0) | |
| Race | | | 0.071 |
| Black or African American (n, %) | 1 (14.3) | 9 (60.0) | |
| White or Caucasian (n, %) | 6 (85.7) | 5 (33.3) | |
| Other (n, %) | 0 (0.0) | 1 (6.7) | |
| Smoking Status | | | 0.384 |
| Current Smoker (n, %) | 0 (0.0) | 0 (0.0) | |
| Previous Smoker (n, %) | 4 (57.1) | 6 (40.0) | |
| Never Smoker (n, %) | 3 (42.9) | 9 (60.0) | |
| Alcohol Use | | | 0.267 |
| Current Alcohol User (n, %) | 3 (42.9) | 1 (6.7) | |
| Previous Alcohol User (n, %) | 0 (0.0) | 2 (13.3) | |
| Never Alcohol User (n, %) | 4 (57.1) | 12 (80.0) | |
| BMI (kg/m2) | 30.0 ± 8.8 | 31.4 ± 7.8 | 0.712 |
| SpO2 (%) | 95.86 ± 2.85 | 96.87 ± 1.92 | 0.581 |
| ICU Admission at Time of Diagnosis (n, %) | 5 (71.4) | 2 (13.3) | 0.014 |
| Ventilator Use in Hospital (n, %) | 5 (71.4) | 6 (40) | 0.361 |
| Corticosteroid Treatment* | 7 (100.0) | 10 (66.7) | 0.135 |

Note: Data are presented as mean ± standard deviation or number of participants with percentage. BMI = Body Mass Index, COPD = Chronic Obstructive Pulmonary Disease, ILD = Interstitial Lung Disease.*, Patients were treated with dexamethasone/methylprednisolone at the diagnosis of COVID-19.

**Table 2**
Symptoms of COVID-19 and comorbidities in Decline and Stable groups at the time of COVID-19 diagnosis.

| Symptoms | Decline Group (n = 7) | Stable Group (n = 15) | p-value |
|---|---|---|---|
| Fever (n, %) | 3 (42.9) | 11 (73.3) | 0.182 |
| Chills (n, %) | 2 (28.6) | 3 (20.0) | 0.523 |
| Cough (n, %) | 4 (44.4) | 11 (73.3) | 0.387 |
| Dyspnea (n, %) | 5 (71.4) | 10 (66.7) | 0.613 |
| Chest pain (n, %) | 2 (28.6) | 4 (26.7) | 0.651 |
| Sore throat (n, %) | 1 (14.3) | 2 (13.3) | 1.000 |
| Fatigue (n, %) | 6 (85.7) | 7 (46.7) | 0.101 |
| Lightheadedness (n, %) | 2 (28.6) | 4 (26.7) | 0.651 |
| Dizziness (n, %) | 1 (14.3) | 2 (13.3) | 1.000 |
| Weakness (n, %) | 0 (0.0) | 3 (20.0) | 0.295 |
| Headache (n, %) | 3 (42.9) | 8 (53.3) | 0.500 |
| Rhinorrhea (n, %) | 1 (14.3) | 2 (13.3) | 1.000 |
| Nasal congestion (n, %) | 1 (14.3) | 3 (20.0) | 1.000 |
| dysgeusia (n, %) | 0 (0.0) | 1 (6.7) | 1.000 |
| Myalgia (n, %) | 2 (28.6) | 5 (33.3) | 0.613 |
| Arthralgia (n, %) | 1 (14.3) | 1 (6.7) | 0.545 |
| Urinary symptoms (n, %) | 0 (0.0) | 1 (6.7) | 1.000 |
| Abdominal pain (n, %) | 2 (28.6) | 3 (20.0) | 0.523 |
| Nausea (n, %) | 1 (14.3) | 3 (20.0) | 1.000 |
| Vomiting (n, %) | 0 (0.0) | 1 (6.7) | 1.000 |
| Diarrhea (n, %) | 3 (42.9) | 2 (13.3) | 0.274 |
| Change in appetite (n, %) | 1 (14.3) | 2 (13.3) | 1.000 |

Note: Data are presented as the number of participants and percentage.

higher absolute neutrophil count (ANC; 5.73 ± 2.68 × $10^9$/L vs. 3.43 ± 1.74 × $10^9$/L; p = 0.031), and lower proportion of lymphocytes (9.90 ± 4.20 % vs. 21.21 ± 10.97 %; p = 0.018) in the Decline group vs. the Stable group on complete blood count (CBC) (Table 3 and Fig. 3A–C). There were no significant differences between the cohorts in white blood cell count (x$10^9$/L; p = 0.082), red blood cell (RBC) count (x$10^{12}$/L; p = 0.902), hemoglobin (g/dL; p = 0.414), hematocrit (%; p = 0.440), platelet count (x$10^9$/L; p = 0.524), RBC distribution width (%; p = 0.992), D-dimer level (mg/L; p = 0.831), C-reactive protein level (mg/dL; p = 0.146), or proportion of monocytes (%; p = 0.094), eosinophils (%; p = 0.615), or basophils (%; p = 0.225) on CBC (Table 3).

### 3.3. CT evaluation

CT evaluation revealed a significantly higher extent of lung involvement of ground-glass opacities (GGO) at follow-up [% lung involvement; 8.50(4.50,14.50) vs. 3.0(1.50,9.50); p = 0.032] and a significantly higher extent of reticulations at baseline [% lung

**Table 3**
Laboratory blood test results at the time of COVID-19 diagnosis.

| Test Result | Decline Group (n = 7) | Stable Group (n = 15) | p-value |
|---|---|---|---|
| White Blood Cell Count (x$10^9$/L) | 7.24 ± 3.30 | 5.15 ± 1.94 | 0.082 |
| Red Blood Cell Count (x$10^{12}$/L) | 3.97 ± 0.30 | 4.01 ± 0.79 | 0.902 |
| Hemoglobin (g/dL) | 11.29 ± 1.07 | 11.91 ± 1.83 | 0.414 |
| Hematocrit (%) | 35.40 ± 2.40 | 37.24 ± 5.87 | 0.440 |
| Neutrophils (%)* | 79.47 ± 4.83 | 65.45 ± 10.22 | 0.003 |
| Lymphocytes (%)* | 9.90 ± 4.20 | 21.21 ± 10.97 | 0.018 |
| Monocytes (%) | 8.49 ± 3.90 | 11.63 ± 3.73 | 0.094 |
| Eosinophils (%) | 0.94 ± 1.14 | 0.74 ± 0.66 | 0.615 |
| Basophils (%) | 0.23 ± 0.18 | 0.34 ± 0.19 | 0.225 |
| Platelet Count (x$10^9$/L) | 221.29 ± 79.55 | 203.79 ± 45.12 | 0.524 |
| ANC (x$10^9$/L)* | 5.73 ± 2.68 | 3.43 ± 1.74 | 0.031 |
| RBC Distribution Width (%) | 14.99 1.79 | 14.98 ± 1.25 | 0.992 |
| D-Dimer (mg/L) | 1.75 ± 1.43 | 1.58 ± 1.88 | 0.831 |
| CRP (mg/dL) | 5.55 ± 6.26 | 2.62 ± 2.41 | 0.146 |

Note: Data are presented as mean ± standard deviation.* = p-value less than 0.05. ANC = Absolute Neutrophil Count, RBC = Red Blood Cell, CRP=C-Reactive Protein.

**Table 4**
Comparison of CT findings between Decline and Stable groups.

| CT Findings | Baseline (%lung involvement) | | p-value | Follow-up (%lung involvement) | | p-value |
|---|---|---|---|---|---|---|
| | Decline Group (n = 7) | Stable Group (n = 15) | | Decline Group (n = 7) | Stable Group (n = 15) | |
| Ground-Glass Opacities* | 15.36 ± 6.44 | 9.03 ± 7.26 | 0.066 | 10.07 ± 5.51 | 4.90 ± 5.13 | 0.032 |
| Traction Bronchiectasis | 2.64 ± 2.21 | 2.20 ± 3.97 | 0.142 | 5.71 ± 4.54 | 4.33 ± 7.95 | 0.091 |
| Subpleural Curvilinear Opacities | 0.71 ± 1.50 | 0.47 ± 1.13 | 0.783 | 0.36 ± 0.75 | 0.17 ± 0.36 | 0.731 |
| Reticulation*# | 7.14 ± 4.37 | 3.40 ± 4.45 | 0.039 | 7.21 ± 5.58 | 3.10 ± 4.36 | 0.041 |
| Consolidation | 4.36 ± 4.91 | 1.43 ± 2.70 | 0.210 | 3.00 ± 2.83 | 1.27 ± 2.43 | 0.185 |
| Honeycombing | 1.43 ± 3.56 | 0.43 ± 0.82 | 0.891 | 1.43 ± 3.56 | 0.43 ± 0.82 | 0.891 |

Note: Data are presented as mean ± standard deviation. # = p-value less than 0.05 at baseline level, * = p-value less than 0.05 at follow-up level. PFT = spirometry Pulmonary Function Testing, CT = Computed Tomography.

**Table 5**
Comparison between baseline and follow-up CT findings.

| CT Findings | Baseline (n = 22) | Follow-up (n = 22) | p-value |
|---|---|---|---|
| Ground-Glass Opacities* | 11.05 ± 7.49 | 6.55 ± 5.68 | 0.004 |
| Traction Bronchiectasis* | 2.34 ± 3.46 | 4.77 ± 6.96 | 0.004 |
| Subpleural Curvilinear Opacities | 0.55 ± 1.22 | 0.23 ± 0.51 | 0.064 |
| Reticulation | 4.59 ± 4.67 | 4.41 ± 5.04 | 0.641 |
| Consolidation | 2.36 ± 3.70 | 1.82 ± 2.63 | 0.362 |
| Honeycombing | 0.75 ± 2.07 | 0.75 ± 2.07 | n/a |

Note: Data are presented as mean ± standard deviation. * = p-value less than 0.05. CT = Computed Tomography.

involvement; 6.50(4.00,9.00) vs. 2.00(0.00,6.00); p = 0.039] and at follow-up [5.00(3.00,13.00) vs. 2.00(0.00,5.00); p = 0.041] in the Decline group vs. the Stable group (Fig. 3, D-F). There were no significant differences observed between cohorts in extent of GGOs at baseline (p = 0.066), traction bronchiectasis at baseline (p = 0.142) or follow-up (p = 0.091), subpleural curvilinear opacities at baseline (p = 0.783) or follow-up (p = 0.731), consolidation at baseline (p = 0.210) or follow-up (p = 0.185), or honeycombing at baseline (p = 0.891) or follow-up (p = 0.891) (Table 4).

When comparing follow-up vs. baseline CT imaging overall, follow-up imaging revealed significantly less lung involvement of GGOs [10.50(3.75,18.25) vs. 4.50(2.00,10.63); p = 0.004] and significantly more of traction bronchiectasis [1.00(0.00,3.63) vs. 2.00 (0.00,8.00); p = 0.004]. Analysis did not reveal significant differences between baseline and follow-up scans in lung involvement of subpleural curvilinear opacities (p = 0.064), reticulations (p = 0.641), consolidation (p = 0.362), or honeycombing (p = 1.000) (Table 5). ICC analysis revealed good consistency between the two radiologists in interpretation of baseline (ICC = 0.931; p < 0.001) and follow-up scans (ICC = 0.930; p < 0.001).

### *3.4. Example CT evaluations*

Fig. 4 shows examples of baseline and follow-up CT image evaluation for two subjects from the Stable and Decline groups. Case 1 is a 47-year-old female patient from the Stable group whose baseline CT demonstrates scattered GGOs (Fig. 4A), significantly diminished on the follow-up CT (Fig. 4B). Case 2 is a 73-year-old male patient from the Decline group whose CT shows evidence of honeycombing,

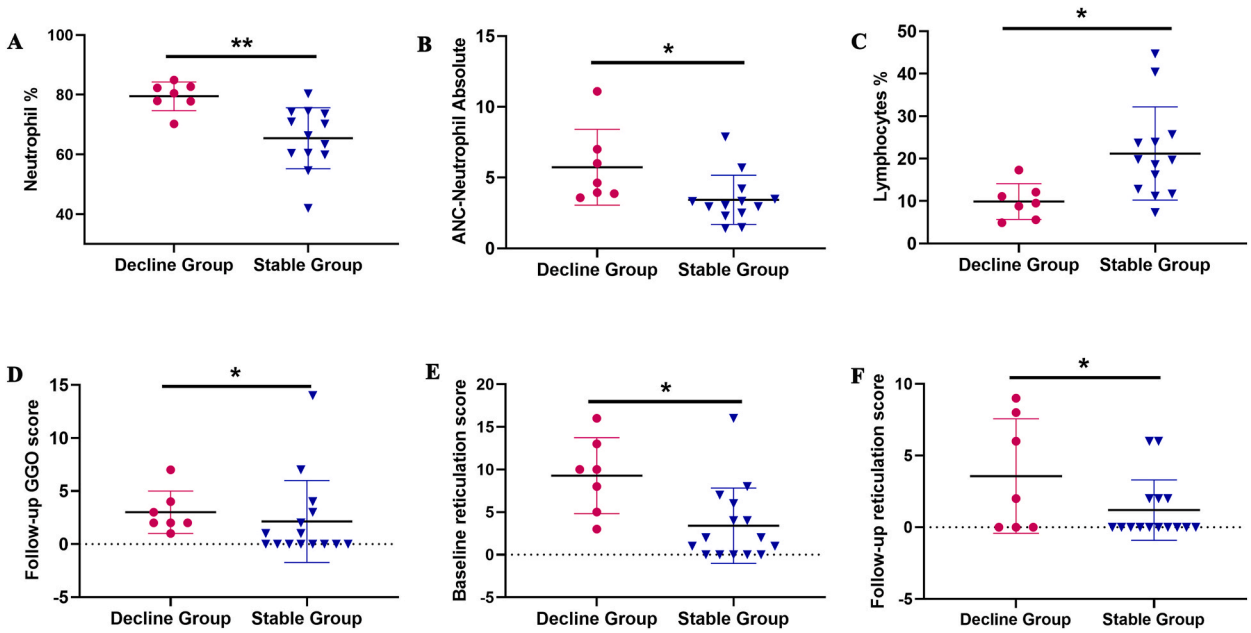


**Fig. 3.** Comparison of laboratory blood test results between Decline and Stable groups: **(A)** percent neutrophils, **(B)** Absolute Neutrophil Count (ANC), and **(C)** percent lymphocytes. Comparison of computed tomographic (CT) findings between Decline and Stable groups: **(D)** follow-up ground-glass opacity (GGO) scores, **(E)** baseline reticulation scores, and **(F)** follow-up reticulation scores. * = p-value <0.05, ** = p-value <0.005.

reticulations, and GGOs at baseline (Fig. 4C). Follow-up CT shows a decrease in GGOs but an increase in honeycombing and reticulations (Fig. 4D).

## 4. Discussion

For patients receiving serial PFT studies for stable underlying pulmonary disease, our findings revealed that elevated neutrophil counts, reduced lymphocyte counts, and substantial burden of pulmonary reticulations observed on chest CT at the time of COVID-19 diagnosis emerged as factors associated with decreased pulmonary function during follow-up. Notably, individuals categorized in the Decline group exhibited a higher prevalence of ground-glass opacities (GGOs) and reticulations on follow-up CT scans compared to those in the Stable group, suggesting a potential association between the severity of acute lung injury during the active phase of COVID-19 and the development of sustained post-COVID lung fibrosis.

Observations about neutrophil and lymphocyte counts in this study underscore the intricate interplay between systemic inflammation and immune response in the long-COVID condition. Evidence from the literature has shown that neutrophils release an inflammatory protease called neutrophil elastase (NE), detected in the airways of patients with cystic fibrosis [29]. An inverse correlation between the levels of free NE in sputum and $FEV_1$ in patients with lung fibrosis has also been demonstrated [30]. One speculation is that elevated NE from increased neutrophils may contribute to decreased $FEV_1$ due to endothelial damage in follow-up COVID-19 patients [31]. On the other hand, lymphopenia has also been demonstrated in patients with long-COVID in other studies [32,33]. Similar results have also been confirmed in primary Sjogren's syndrome associated ILD [34]. There is evidence indicating that cytokines such as interleukin (IL)-4, IL-13, and transforming growth factor (TGF)-β can promote pulmonary fibrosis through fibroblast proliferation, activation, and collagen production [35,36]. Previous studies have identified elevated levels of cytokines in the lung in comparison to peripheral circulation [37,38]. These elevated cytokines may induce lymphocyte migration from peripheral circulation to lung tissue, resulting in fewer lymphocytes in the peripheral blood in patients with long-COVID, exacerbating development of pulmonary fibrosis and decreased pulmonary function [39].

This study suggests that higher baseline burden of reticulation on chest CT may be associated with long-COVID lung fibrosis and decline in pulmonary function. The persistence of radiological abnormalities, such as reticulations, beyond the acute phase of the disease may signify ongoing pulmonary remodeling and fibrotic changes, contributing to the observed decline in pulmonary function. Reticulation is one of the main CT findings indicative of pulmonary fibrosis and has previously been identified in long-COVID subjects [40,41]. Several studies also documented the appearance of GGOs and reticulations in patients after 1 year of recovery from COVID-19 [24,42]. Furthermore, after minimizing the cofounder of pre-existing pulmonary disease, a higher prevalence of GGOs on follow-up chest CT was shown in the group with decreased pulmonary function, which indicates GGOs may persist for a longer duration in patients experiencing long-COVID symptoms. Our findings suggest a potential explanation for the variability observed in ground-glass opacity abnormalities across studies [22,23], highlighting the need for further investigation to determine the duration required for complete resolution of GGO and then improve the consistency and comparability of future studies. Additionally, clinicians should be

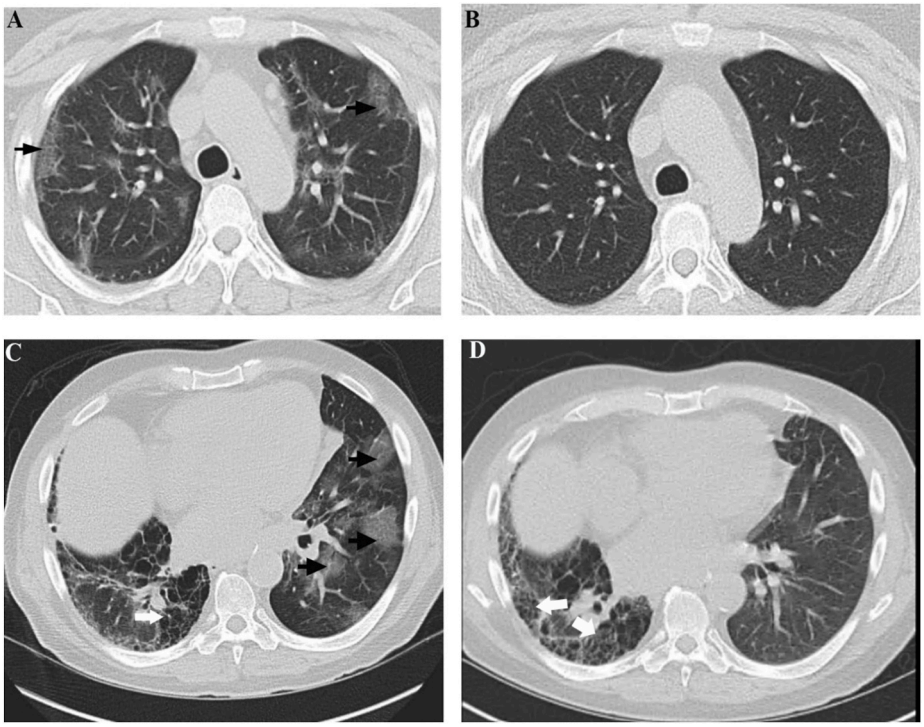


**Fig. 4.** Examples of baseline and follow-up CT image evaluations from the Stable (**A-B**) and Decline (**C-D**) groups. In a 47-year-old female patient from the Stable group, scattered ground-glass opacities (GGOs) (black arrows in **A**) are visible but diminish significantly by follow-up (**B**). A 73-year-old male patient from the Decline group has evidence of honeycombing and reticulations (white arrow in **C**), as well as GGOs (black arrows in **C**) at baseline. Upon follow-up, there is a decrease in GGOs (left lung in **D**) but increase in honeycombing and reticulations (white arrow in **D**).

vigilant in monitoring such individuals closely, even after apparent recovery from acute COVID-19, to detect and manage potential sequelae effectively. Additionally, our results highlight the importance of longitudinal follow-up and comprehensive pulmonary function assessments in post-COVID care, particularly among patients with significant radiological findings suggestive of ongoing pulmonary pathology.

Interestingly, our study did not find associations between the presence of selected comorbidities or evaluated symptoms at the time of COVID-19 diagnosis and decreased pulmonary function post-recovery. While these findings may suggest that the impact of COVID-19 on pulmonary function extends beyond the influence of pre-existing medical conditions or acute symptomatic manifestations, further research is warranted to elucidate the complex interactions between host factors, disease severity, and long-term pulmonary outcomes in COVID-19 survivors.

Our study is limited in its retrospective nature and small sample size. Patients were included in the study only if they met stringent inclusion and exclusion criteria. Consequently, many patients admitted to our institution for COVID-19 did not meet study criteria and were not included. It is important to note that this preliminary study represents a control for confounding factors, although it may limit the generalizability of our findings to a broader population of COVID-19 patients. Similarly, this is a single-institution study; larger multi-institution studies are needed to improve generalizability. Future research endeavors should aim to foster collaboration with other medical facilities to broaden the scope of our findings and enhance the generalizability of our results to diverse populations. Our results apply to a specific patient cohort – those with stable underlying pulmonary disease who were monitored by serial PFTs prior to their COVID-19 diagnosis. A portion of these patients may already be predisposed to hospitalization and PFT decline, limiting the generalizability of our findings. Additionally, the requirements for PFT and CT evaluation likely skewed our patient population toward those who required a higher level of care (i.e., ICU admission) during hospitalization. Thus, our methodology may not allow us to elucidate whether declining PFT results were specifically attributable to COVID-19 disease vs. non-COVID-19 acute lung injury experienced by patients [43,44].

## 5. Conclusion

This study underscores the importance of clinical parameters such as neutrophil counts, reduced lymphocyte counts, pulmonary reticulation on chest CT at diagnosis, and extent of GGO on follow-up chest CT in guiding the management of post-COVID-19 patients, particularly those with pre-existing pulmonary conditions. This insight may further the understanding of long-term COVID-19 sequelae, allowing for optimized intervention to mitigate the progression of long-COVID-19. However, it is imperative to acknowledge that further larger-sample research is warranted to better understand long-COVID and its impact on lung function in this patient

population.

## Ethics statement

The study has been approved by the Institutional Review Board of Johns Hopkins (IRB00329311) with a waiver of informed consent from each study participant.

## Funding

This study was supported by BriteStar Award (IO# 80060914).

## Data availability statement

The authors declare that they had full access to all the data in this study and the authors take complete responsibility for the integrity of the data and the accuracy of the data analysis. All data will be made available on request.

## CRediT authorship contribution statement

**Lin-Mei Zhao:** Writing – review & editing, Writing – original draft, Methodology, Data curation, Conceptualization. **Andrew C. Lancaster:** Methodology, Data curation. **Ritesh Patel:** Data curation. **Helen Zhang:** Writing – review & editing. **Tim Q. Duong:** Validation, Supervision. **Zhicheng Jiao:** Supervision, Software, Methodology. **Cheng Ting Lin:** Visualization, Methodology, Investigation. **Terrance Healey:** Writing – review & editing. **Thaddeus Wright:** Writing – review & editing. **Jing Wu:** Visualization, Supervision, Funding acquisition. **Harrison X. Bai:** Writing – review & editing, Supervision, Project administration, Investigation, Funding acquisition, Conceptualization.

## Declaration of competing interest

The authors declare that they have no known competing financial interests or personal relationships that could have appeared to influence the work reported in this paper.

## Acknowledgments

The authors are grateful to all the subjects who participated in this study.

## Appendix A. Supplementary data

Supplementary data to this article can be found online at https://doi.org/10.1016/j.heliyon.2024.e31751.

## References

[1] A. Nalbandian, K. Sehgal, A. Gupta, M.V. Madhavan, C. McGroder, J.S. Stevens, J.R. Cook, A.S. Nordvig, D. Shalev, T.S. Sehrawat, N. Ahluwalia, B. Bikdeli, D. Dietz, C. Der-Nigoghossian, N. Liyanage-Don, G.F. Rosner, E.J. Bernstein, S. Mohan, A.A. Beckley, D.S. Seres, T.K. Choueiri, N. Uriel, J.C. Ausiello, D. Accili, D.E. Freedberg, M. Baldwin, A. Schwartz, D. Brodie, C.K. Garcia, M.S.V. Elkind, J.M. Connors, J.P. Bilezikian, D.W. Landry, E.Y. Wan, Post-acute COVID-19 syndrome, Nat. Med. 27 (4) (2021) 601–615.

[2] D. Montani, L. Savale, N. Noel, O. Meyrignac, R. Colle, M. Gasnier, E. Corruble, A. Beurnier, E.M. Jutant, T. Pham, A.L. Lecoq, J.F. Papon, S. Figueiredo, A. Harrois, M. Humbert, X. Monnet, C.S. Group, Post-acute COVID-19 syndrome, Eur. Respir. Rev. 31 (163) (2022).

[3] M. Michelen, L. Manoharan, N. Elkheir, V. Cheng, A. Dagens, C. Hastie, M. O'Hara, J. Suett, D. Dahmash, P. Bugaeva, I. Rigby, D. Munblit, E. Harriss, A. Burls, C. Foote, J. Scott, G. Carson, P. Olliaro, L. Sigfrid, C. Stavropoulou, Characterising long COVID: a living systematic review, BMJ Glob. Health 6 (9) (2021).

[4] H. Akbarialiabad, M.H. Taghrir, A. Abdollahi, N. Ghahramani, M. Kumar, S. Paydar, B. Razani, J. Mwangi, A.A. Asadi-Pooya, L. Malekmakan, B. Bastani, Long COVID, a comprehensive systematic scoping review, Infection 49 (6) (2021) 1163–1186.

[5] P. Urso, A. Cattaneo, S. Pulvirenti, F. Vercelli, D.M. Cavallo, P. Carrer, Early-phase pandemic in Italy: covid-19 spread determinant factors, Heliyon 9 (4) (2023) e15358.

[6] Q. Han, B. Zheng, L. Daines, A. Sheikh, Long-term sequelae of COVID-19: a systematic review and meta-analysis of one-year follow-up studies on post-COVID symptoms, Pathogens 11 (2) (2022).

[7] E. Baratella, R. Bussani, F. Zanconati, C. Marrocchio, G. Fabiola, L. Braga, S. Maiocchi, G. Berlot, M.C. Volpe, E. Moro, P. Confalonieri, M.A. Cova, M. Confalonieri, F. Salton, B. Ruaro, Radiological-pathological signatures of patients with COVID-19-related pneumomediastinum: is there a role for the Sonic hedgehog and Wnt5a pathways? ERJ Open Res 7 (3) (2021).

[8] L.T. McDonald, Healing after COVID-19: are survivors at risk for pulmonary fibrosis? Am. J. Physiol. Lung Cell Mol. Physiol. 320 (2) (2021) L257–L265.

[9] D. Singh, A.G. Mathioudakis, A. Higham, Chronic obstructive pulmonary disease and COVID-19: interrelationships, Curr. Opin. Pulm. Med. 28 (2) (2022) 76–83.

[10] W. Zhang, H. Wu, Q. Guo, X. Xu, Y. Pu, C. Chen, M. Cao, D. Sun, W. Lu, H. Yi, S. Zhou, B. Fang, Association of clinical characteristics and vaccines with risk of persistently viral clearance in patients infected with SARS-CoV-2 Omicron variant in Shanghai, China, Heliyon 10 (1) (2024) e23256.

[11] L. Huang, Q. Yao, X. Gu, Q. Wang, L. Ren, Y. Wang, P. Hu, L. Guo, M. Liu, J. Xu, X. Zhang, Y. Qu, Y. Fan, X. Li, C. Li, T. Yu, J. Xia, M. Wei, L. Chen, Y. Li, F. Xiao, D. Liu, J. Wang, X. Wang, B. Cao, 1-year outcomes in hospital survivors with COVID-19: a longitudinal cohort study, Lancet 398 (10302) (2021) 747–758.

[12] X. Wu, X. Liu, Y. Zhou, H. Yu, R. Li, Q. Zhan, F. Ni, S. Fang, Y. Lu, X. Ding, H. Liu, R.M. Ewing, M.G. Jones, Y. Hu, H. Nie, Y. Wang, 3-month, 6-month, 9-month, and 12-month respiratory outcomes in patients following COVID-19-related hospitalisation: a prospective study, Lancet Respir. Med. 9 (7) (2021) 747–754.
[13] S. Stanojevic, D.A. Kaminsky, M.R. Miller, B. Thompson, A. Aliverti, I. Barjaktarevic, B.G. Cooper, B. Culver, E. Derom, G.L. Hall, T.S. Hallstrand, J.D. Leuppi, N. MacIntyre, M. McCormack, M. Rosenfeld, E.R. Swenson, ERS/ATS technical standard on interpretive strategies for routine lung function tests, Eur. Respir. J. 60 (1) (2022).
[14] S.A. Guler, L. Ebner, C. Aubry-Beigelman, P.O. Bridevaux, M. Brutsche, C. Clarenbach, C. Garzoni, T.K. Geiser, A. Lenoir, M. Mancinetti, B. Naccini, S.R. Ott, L. Piquilloud, M. Prella, Y.A. Que, P.M. Soccal, C. von Garnier, M. Funke-Chambour, Pulmonary function and radiological features 4 months after COVID-19: first results from the national prospective observational Swiss COVID-19 lung study, Eur. Respir. J. 57 (4) (2021).
[15] D.M. Hansell, A.A. Bankier, H. MacMahon, T.C. McLoud, N.L. Muller, J. Remy, Fleischner Society: glossary of terms for thoracic imaging, Radiology 246 (3) (2008) 697–722.
[16] T.V. Lerum, T.M. Aalokken, E. Bronstad, B. Aarli, E. Ikdahl, K.M.A. Lund, M.T. Durheim, J.R. Rodriguez, C. Meltzer, K. Tonby, K. Stavem, O.H. Skjonsberg, H. Ashraf, G. Einvik, Dyspnoea, lung function and CT findings 3 months after hospital admission for COVID-19, Eur. Respir. J. 57 (4) (2021).
[17] J.H. Lee, J.J. Yim, J. Park, Pulmonary function and chest computed tomography abnormalities 6-12 months after recovery from COVID-19: a systematic review and meta-analysis, Respir. Res. 23 (1) (2022) 233.
[18] M. So, H. Kabata, K. Fukunaga, H. Takagi, T. Kuno, Radiological and functional lung sequelae of COVID-19: a systematic review and meta-analysis, BMC Pulm. Med. 21 (1) (2021) 97.
[19] M. Babar, H. Jamil, N. Mehta, A. Moutwakil, T.Q. Duong, Short- and long-term chest-CT findings after recovery from COVID-19: a systematic review and meta-analysis, Diagnostics 14 (6) (2024).
[20] J. Tarraso, B. Safont, J.A. Carbonell-Asins, E. Fernandez-Fabrellas, J.N. Sancho-Chust, E. Naval, B. Amat, S. Herrera, J.A. Ros, J.J. Soler-Cataluña, Lung function and radiological findings 1 year after COVID-19: a prospective follow-up, Respir. Res. 23 (1) (2022) 242.
[21] X. Han, L. Chen, Y. Fan, O. Alwalid, X. Jia, Y. Zheng, J. Liu, Y. Li, Y. Cao, J. Gu, Longitudinal assessment of chest CT findings and pulmonary function after COVID-19 infection, Radiology 307 (2) (2023) e222888.
[22] A.K. Luger, T. Sonnweber, L. Gruber, C. Schwabl, K. Cima, P. Tymoszuk, A.K. Gerstner, A. Pizzini, S. Sahanic, A. Boehm, Chest CT of lung injury 1 year after COVID-19 pneumonia: the CovILD study, Radiology 304 (2) (2022) 462–470.
[23] F. Pan, L. Yang, B. Liang, T. Ye, L. Li, L. Li, D. Liu, J. Wang, R.L. Hesketh, C. Zheng, Chest CT patterns from diagnosis to 1 year of follow-up in patients with COVID-19, Radiology 302 (3) (2022) 709–719.
[24] M.J. Cha, J.J. Solomon, J.E. Lee, H. Choi, K.J. Chae, K.S. Lee, D.A. Lynch, Chronic lung injury after COVID-19 pneumonia: clinical, radiologic, and histopathologic perspectives, Radiology 310 (1) (2024) e231643.
[25] H. Robbie, A.U. Wells, J. Jacob, S.L.F. Walsh, A. Nair, A. Srikanthan, P. Tazoniero, A. Devaraj, Visual and automated CT measurements of lung volume loss in idiopathic pulmonary fibrosis, AJR Am. J. Roentgenol. 213 (2) (2019) 318–324.
[26] J.M. Oldham, C.T. Lee, Z. Wu, W.S. Bowman, J.V. Pugashetti, N. Dao, J. Tonkin, H. Seede, G. Echt, A. Adegunsoye, F. Chua, T.M. Maher, C.K. Garcia, M.E. Strek, C.A. Newton, P.L. Molyneaux, Lung function trajectory in progressive fibrosing interstitial lung disease, Eur. Respir. J. 59 (6) (2022).
[27] M.S. Durstenfeld, K. Sun, P. Tahir, M.J. Peluso, S.G. Deeks, M.A. Aras, D.J. Grandis, C.S. Long, A. Beatty, P.Y. Hsue, Use of cardiopulmonary exercise testing to evaluate long COVID-19 symptoms in adults: a systematic review and meta-analysis, JAMA Netw. Open 5 (10) (2022) e2236057.
[28] M. Francone, F. Iafrate, G.M. Masci, S. Coco, F. Cilia, L. Manganaro, V. Panebianco, C. Andreoli, M.C. Colaiacomo, M.A. Zingaropoli, M.R. Ciardi, C. M. Mastroianni, F. Pugliese, F. Alessandri, O. Turriziani, P. Ricci, C. Catalano, Chest CT score in COVID-19 patients: correlation with disease severity and short-term prognosis, Eur. Radiol. 30 (12) (2020) 6808–6817.
[29] J.A. Voynow, M. Shinbashi, Neutrophil elastase and chronic lung disease, Biomolecules 11 (8) (2021).
[30] S.D. Sagel, R. Kapsner, I. Osberg, M.K. Sontag, F.J. Accurso, Airway inflammation in children with cystic fibrosis and healthy children assessed by sputum induction, Am. J. Respir. Crit. Care Med. 164 (8 Pt 1) (2001) 1425–1431.
[31] H. Ng, S. Havervall, A. Rosell, K. Aguilera, K. Parv, F.A. von Meijenfeldt, T. Lisman, N. Mackman, C. Thalin, M. Phillipson, Circulating markers of neutrophil extracellular traps are of prognostic value in patients with COVID-19, Arterioscler. Thromb. Vasc. Biol. 41 (2) (2021) 988–994.
[32] M.S. Rha, E.C. Shin, Activation or exhaustion of CD8(+) T cells in patients with COVID-19, Cell. Mol. Immunol. 18 (10) (2021) 2325–2333.
[33] G.C. Lechuga, C.M. Morel, S.G. De-Simone, Hematological alterations associated with long COVID-19, Front. Physiol. 14 (2023) 1203472.
[34] L. Shi, J. Wang, H.X. Guo, X.L. Han, Y.P. Tang, G.Y. Liu, Circulating Th2 cell reduction and Th1/Th2 imbalance are correlated with primary Sjogren's syndrome-associated interstitial lung disease, Arthritis Res. Ther. 24 (1) (2022) 121.
[35] K. Izuhara, S. Nunomura, Y. Nanri, M. Ogawa, J. Ono, Y. Mitamura, T. Yoshihara, Periostin in inflammation and allergy, Cell. Mol. Life Sci. 74 (23) (2017) 4293–4303.
[36] F.Q. Wen, T. Kohyama, X. Liu, Y.K. Zhu, H. Wang, H.J. Kim, T. Kobayashi, S. Abe, J.R. Spurzem, S.I. Rennard, Interleukin-4- and interleukin-13-enhanced transforming growth factor-beta2 production in cultured human bronchial epithelial cells is attenuated by interferon-gamma, Am. J. Respir. Cell Mol. Biol. 26 (4) (2002) 484–490.
[37] T. Kimura, Y. Ishii, K. Yoh, Y. Morishima, T. Iizuka, T. Kiwamoto, Y. Matsuno, S. Homma, A. Nomura, T. Sakamoto, S. Takahashi, K. Sekizawa, Overexpression of the transcription factor GATA-3 enhances the development of pulmonary fibrosis, Am. J. Pathol. 169 (1) (2006) 96–104.
[38] P. Pignatti, G. Brunetti, D. Moretto, M.R. Yacoub, M. Fiori, B. Balbi, A. Balestrino, G. Cervio, S. Nava, G. Moscato, Role of the chemokine receptors CXCR3 and CCR4 in human pulmonary fibrosis, Am. J. Respir. Crit. Care Med. 173 (3) (2006) 310–317.
[39] C. Giacomelli, R. Piccarducci, L. Marchetti, C. Romei, C. Martini, Pulmonary fibrosis from molecular mechanisms to therapeutic interventions: lessons from post-COVID-19 patients, Biochem. Pharmacol. 193 (2021) 114812.
[40] T. Franquet, A. Gimenez, L. Ketai, S. Mazzini, A. Rial, V. Pomar, P. Domingo, Air trapping in COVID-19 patients following hospital discharge: retrospective evaluation with paired inspiratory/expiratory thin-section CT, Eur. Radiol. 32 (7) (2022) 4427–4436.
[41] Y. Zheng, L. Wang, S. Ben, Meta-analysis of chest CT features of patients with COVID-19 pneumonia, J. Med. Virol. 93 (1) (2021) 241–249.
[42] A. Watanabe, M. So, M. Iwagami, K. Fukunaga, H. Takagi, H. Kabata, T. Kuno, One-year follow-up CT findings in COVID-19 patients: a systematic review and meta-analysis, Respirology 27 (8) (2022) 605–616.
[43] P.J. Ohtake, A.C. Lee, J.C. Scott, R.S. Hinman, N.A. Ali, C.R. Hinkson, D.M. Needham, L. Shutter, H. Smith-Gabai, M.C. Spires, A. Thiele, C. Wiencek, J.M. Smith, Physical impairments associated with post-intensive care syndrome: systematic review based on the world health organization's international classification of functioning, disability and health framework, Phys. Ther. 98 (8) (2018) 631–645.
[44] J.R. Masclans, O. Roca, X. Munoz, E. Pallisa, F. Torres, J. Rello, F. Morell, Quality of life, pulmonary function, and tomographic scan abnormalities after ARDS, Chest 139 (6) (2011) 1340–1346.